

29
1-28-81
2567.15
R

(2)

R-1518

UCC-ND

ORNL/CSD/TM-144

MASTER

NUCLÉAR
DIVISION



**Analysis and Solution of
the Ill-posed Inverse Heat
Conduction Problem**

Charles F. Weber

OPERATED BY
UNION CARBIDE CORPORATION
FOR THE UNITED STATES
DEPARTMENT OF ENERGY

ORNL/CSD/TM-144

**ANALYSIS AND SOLUTION OF THE ILL-POSED
INVERSE HEAT CONDUCTION PROBLEM**

Charles F. Weber

**Sponsor: D. G. Cacuci
Engineering Physics Division**

Date Published - January 1981

**COMPUTER SCIENCE DIVISION
at
Oak Ridge National Laboratory
Post Office Box X
Oak Ridge, Tennessee 37830**

NOTICE This document contains information of a preliminary nature
It is subject to revision or correction and therefore does not represent a
final report.

**Union Carbide Corporation, Nuclear Division
operating the
Oak Ridge Gaseous Diffusion Plant • Paducah Gaseous Diffusion Plant
Oak Ridge Y-12 Plant • Oak Ridge National Laboratory
under Contract No. W-7405-eng-26
for the
Department of Energy**

Rey

TABLE OF CONTENTS

	<u>Page</u>
LIST OF TABLES	v
LIST OF FIGURES.	vii
ACKNOWLEDGMENTS.	ix
ABSTRACT	xi
I. INTRODUCTION	1
II. ILL-POSEDNESS OF THE INVERSE HEAT CONDUCTION PROBLEM	4
III. GENERAL SOLUTION PROCEDURE	7
IV. SAMPLE PROBLEMS.	10
V. NUMERICAL APPROXIMATIONS	14
VI. COMPUTATION RESULTS.	16
VII. SUMMARY AND CONCLUSIONS.	24
REFERENCES	27
APPENDIX	29

LIST OF TABLES

	<u>Page</u>
1. <i>Problem III</i> Radial Profile Comparison of Calculated and Exact Temperatures Solution at Selected Time Values.	17
2. <i>Problem I</i> Surface Calculations	18
3. <i>Problem II</i> Surface Calculations.	19
4. <i>Problem III</i> Surface Calculations with Exponential Decrease in Exact Solution	20
5. <i>Problem III</i> Surface Calculations with Exponential Increase in Exact Solution	21
6. <i>Problem II</i> Surface Temperature Results with Perturbed Data . . .	22

LIST OF FIGURES

	<u>Page</u>
1. Diagram of Direct and Inverse Problem Regions.	2
2. Characteristic Curves of Modified System	9

ACKNOWLEDGMENTS

This study was supported by the Nuclear Regulatory Commission through the Oak Ridge National Laboratory Pressurized Water Reactor-Blowdown Heat Transfer Separate Effects Program. The author greatly appreciates the support and suggestions of Dan Cacuci, Paul Mandlin, and Cecil Parks. Special thanks are due to Pam Young for the expert and patient typing of the many drafts of this paper.

ABSTRACT

The inverse conduction problem arises when experimental measurements are taken in the interior of a body, and it is desired to calculate temperature and heat flux values on the surface. The problem is shown to be ill-posed, as the solution exhibits unstable dependence on the given data functions. A special solution procedure is developed for the one-dimensional case which replaces the heat conduction equation with an approximating hyperbolic equation. If viewed from a new perspective, where the roles of the spatial and time variables are interchanged, then an initial value problem for the damped wave equation is obtained. Since this formulation is well-posed, both analytic and numerical solution procedures are readily available. Sample calculations confirm that this approach produces consistent, reliable results for both linear and nonlinear problems.

**ANALYSIS AND SOLUTION OF THE ILL-POSED
INVERSE HEAT CONDUCTION PROBLEM**

C. F. Weber

I. INTRODUCTION

The classical direct problem in heat conduction is to determine the interior temperature distribution of a body from data given on its surface. However, applications arise in which data is not available over the entire surface but is given instead at interior points. In such cases, it is necessary to calculate surface temperatures rather than use them to calculate interior values. This constitutes an *inverse problem*.

Consider, for example, the illustration in Fig. 1. Boundary conditions given at x' and x'' result in a direct problem for $x' \leq x \leq x''$ and inverse problems in the regions where $0 \leq x \leq x'$ or $x'' \leq x \leq L$. If x' and x'' coincide, then two independent conditions (e.g., temperature and heat flux) must be specified, and two inverse problems exist. If x' and x'' are different points, then the direct problem is solved first and its solution used to obtain boundary conditions for each inverse problem.

Analysis of the direct problem has progressed for almost two centuries, resulting in a wealth of knowledge concerning the behavior of both exact and numerical solution procedures. Because this problem is well-posed, solution computations are straightforward, even for nonlinear problems and irregular geometries. Unfortunately, the same is not true for the inverse problem. The ill-posed nature of this problem not only

ORNL-DWG 80-14612

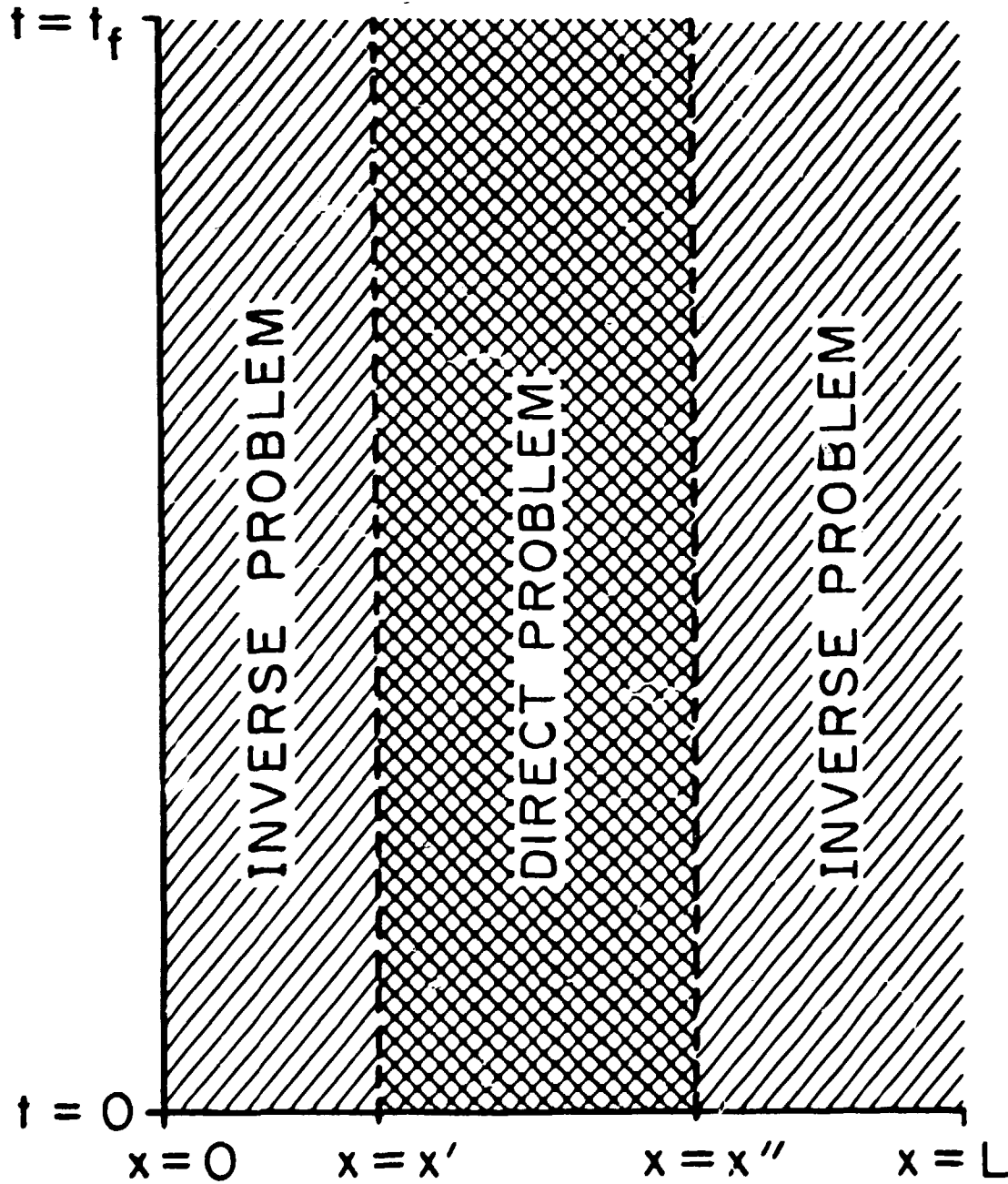


Fig. 1. Diagram of Direct and Inverse Problem Regions

defies easy solution, but serves to discourage the type of massive study that has accompanied the direct problem.

Present methods of solving the inverse conduction problem include exact, integral, and discrete numerical techniques. Exact and integral methods [1,2] have contributed significantly to the theory and understanding of the problem, but are usually restricted to applications with constant physical properties. Discrete approximation by finite differences [3,4,5] or finite elements [6] are applicable to nonlinear problems, but the success of these methods is still limited in many cases by the inherent ill-posedness of the problem. Although good results have been obtained in some situations, discrete methods are generally not capable of handling more complicated problems without some corrective action.

As a result, various improvements in conventional discrete methods have been proposed. Garifo, Schrock, and Spedicato [4] describe a procedure to approximate the actual solution by solving a sequence of well-posed problems. Good results are obtained for some cases, although the authors note certain situations where the method fails completely. Favorable results have also been achieved by Beck [3] using nonlinear estimation. In this method, accurate surface flux values are determined by a least squares procedure which calculates a correction from previously computed (but possibly inaccurate) temperature values. This is probably the most successful and consistent approach currently in use.

An alternate procedure is described in this article which uses a technique similar to the *quasi-inversion* principle described by Tikhonov and Arsenin [7]. In this approach, the inverse problem is closely approximated by a well-posed problem whose solution is easily obtained.

In addition, a great wealth of knowledge exists concerning the behavior of this new problem and stable, high order numerical methods are already available.

To better understand the difficulties inherent in the inverse problem, a detailed analysis of its ill-posed nature is carried out in Sect. II. The general solution procedure is then described in Sect. III. Sect. IV presents three sample problems, representing slab and radial geometries, as well as constant and temperature dependent physical properties. In Sect. V, the solution technique is applied to the sample problems, and the resulting approximations are discretized to obtain numerical solutions. These numerical results are reported in Sect. VI and compared to the known exact solutions. Finally, Sect. VII provides a summary and conclusions.

II. ILL-POSEDNESS OF THE INVERSE HEAT CONDUCTION PROBLEM

The concept of a *well-posed* problem* was first introduced by J. Hadamard in 1923, and has been developed significantly since then. There is a general consensus that a well-posed problem is one for which a solution exists, is unique, and depends continuously on given data. This last condition, termed *stability*, ensures that small changes in data will produce small changes in the solution.

The inverse conduction problem has been considered ill-posed by several authors [3,4]. To undertake a further analysis, consider the heat conduction equation in slab geometry with constant physical properties,

*The information in this paragraph is adapted largely from both the translation editor's preface and the author's preface to the English edition [7].

$$\frac{\partial T}{\partial t} - \alpha \frac{\partial^2 T}{\partial x^2} = Q(x, t), \quad 0 < x < L, \quad 0 < t < t_f, \quad (1a)$$

where $\alpha = k/\rho C_p$ is the thermal diffusivity. Referring to Fig. 1, an inverse problem arises when auxiliary conditions occur in the form

$$T(x^-, t) = f(t) \quad (1b)$$

$$\frac{\partial T}{\partial x}(x^-, t) = g(t) \quad (1c)$$

$$T(x, 0) = T_0(x). \quad (1d)$$

For the special case where $x^+ = x^- = 0$ and $Q(x, t) = 0$, Burggraf [1] has shown that if f and g are infinitely differentiable, then the solution to Eqs. (1a) - (1c) is given by

$$T(x, t) = \sum_{n=0}^{\infty} \frac{1}{(2n)!} \left(\frac{x^2}{\alpha}\right)^n f^{(n)}(t) - \frac{x}{k} \sum_{n=0}^{\infty} \frac{1}{(2n+1)!} \left(\frac{x^2}{\alpha}\right)^n g^{(n)}(t). \quad (2)$$

This result is also obtained by Widder [8], who formally proves existence of this solution by showing that both series in Eq. (2) converge uniformly for bounded t , provided that f and g satisfy

$$\left| f^{(n)}(t) \right| \leq M \frac{(2n)!}{L^n}, \quad \text{and} \quad \left| g^{(n)}(t) \right| \leq P \frac{(2n)!}{L^n}, \quad n = 0, 1, 2, \dots,$$

for some constants M and P . Uniqueness of the solution (2) follows quickly since any two solutions must both be equal to the right-hand side of Eq. (2), and therefore to each other.

In many applications, the initial temperature T_0 is determined from a steady-state problem using $f(0)$ and $g(0)$ as input. For other situations, T_0 may be determined separately. In any case, if the initial condition T_0 satisfies the compatibility condition

$$T_0'(x) = \sum_{n=0}^{\infty} \frac{1}{(2n)!} \left(\frac{x^2}{\alpha}\right)^n f^{(n)}(0) - \frac{x}{k} \sum_{n=0}^{\infty} \frac{1}{(2n+1)!} \left(\frac{x^2}{\alpha}\right)^n g^{(n)}(0), \quad (3)$$

then the solution at any point depends continuously on the initial

temperature. However, even if Eq. (3) does hold, it will be shown that Eq. (2) does not depend continuously on f and g .

In examining the stability of the solution (2), it is necessary to measure the differences between two sets of data and the differences between corresponding solutions. For this purpose, consider the maximum-norms for both data and solution,

$$\|f\| = \max_{0 \leq t \leq t_f} |f(t)|, \quad \|g\| = \max_{0 \leq t \leq t_f} |g(t)|, \quad \|T\| = \max_{\substack{0 \leq x \leq L \\ 0 \leq t \leq t_f}} |T(x,t)|. \quad (4)$$

Now, let $T_1(x,t)$ and $T_2(x,t)$ be solutions of Eq. (2) resulting from the temperature and flux data $f_1(t)$, $g_1(t)$ and $f_2(t)$, $g_2(t)$, respectively. A necessary condition for stability is that the norm $\|T_1 - T_2\|$ can be made arbitrarily small by choosing f_1 , f_2 , g_1 , and g_2 so that the norms $\|f_1 - f_2\|$ and $\|g_1 - g_2\|$ are sufficiently small. This is generally impossible, as can be seen by the following example.

Let $g_1 = g_2 = 0$ and let f_1 be an arbitrary analytic function. For a second data function $f_2(t) = f_1(t) + \frac{1}{\beta} \cos \beta^2 t$, $\beta^2 > 0$, the "error term" $\frac{1}{\beta} \cos \beta^2 t$ can be made arbitrarily small by picking β large enough. This forces f_1 and f_2 to be arbitrarily "close," as measured by the norm of Eq. (4), since

$$\|f_1 - f_2\| = \max_{0 \leq t \leq t_f} \left| \frac{1}{\beta} \cos \beta^2 t \right| = \frac{1}{\beta}.$$

However, as detailed in the Appendix, the corresponding solutions T_1 and T_2 may not be close at all, since

$$\|T_1 - T_2\| \geq \frac{1}{\beta} \left| \sum_{n=0}^{\infty} \frac{(-1)^n}{(4n)!} \beta^{4n} \right| = \frac{1}{\beta} \left| \cosh \frac{\beta}{\sqrt{2}} \cos \frac{\beta}{\sqrt{2}} \right|. \quad (5)$$

Because the term on the far right is unbounded in β , a small data norm will never result in a small solution norm; hence, the solution (2) is unstable.

III. GENERAL SOLUTION PROCEDURE

Because of the unstable solution dependence on boundary data, the approach in Sect. II is totally inadequate for most practical problems. A truly satisfactory solution must remain stable even if data is given approximately.

The alternative procedure presented here slightly alters system (1) so as to produce a well-posed system. This new system will yield a solution which is a good approximation to the desired solution of the ill-posed problem. This procedure (called quasi-inversion) resembles the use of artificial viscosity terms to smooth out shock discontinuities in fluid mechanics problems [9]. The technique is also mentioned by Tikhonov and Arsenin [7], who briefly discuss the approach for a general nonlinear ill-posed system.

Following this approach, consider the system

$$\gamma \frac{\partial^2 T}{\partial t^2} + \frac{\partial T}{\partial t} - \alpha \frac{\partial^2 T}{\partial x^2} = 0 \quad 0 < x < L, \quad 0 < t < t_f. \quad (6a)$$

$$T(x, 0) = T_0(x) \quad (6b)$$

$$T(0, t) = f(t) \quad (6c)$$

$$\frac{\partial T}{\partial x}(0, t) = g(t) \quad (6d)$$

$$T(x, t_f) = T_1(x), \quad (6e)$$

where γ is a non-negative constant and T_1 is an arbitrary function. If γ is small, then Eq. (6a) closely resembles Eq. (1a). In fact, Morse and Feshbach [10] suggest this (the "telegraph" equation) as a better model of heat conduction, since it does not permit instantaneous transfer of heat as Eq. (1a) does. For $\gamma > 0$, Eq. (6a) is hyperbolic and has a solution resembling traveling waves. The characteristics of this equation are lines with slopes $\pm \sqrt{\gamma/\alpha}$, as depicted in Fig. 2. Because the domain of dependence for the solution at any point is bounded by the characteristics through that point, the additional boundary condition Eq. (6e) affects only the shaded region of Fig. 2. For small enough γ , the size of this region becomes insignificant; hence, the effects of Eq. (6e) can largely be eliminated.* Thus, for small γ , system (6) closely approximates the actual inverse system (1).

In his development of nonlinear estimation, Beck [3] notes that the surface heat flux at time t depends on interior temperature values at times both before and after t . Although this may appear to violate physical intuition, it is a fundamental concept that will allow an efficient, stable solution of system (8).

The hyperbolic system (6) involves only one space variable and is to be solved in the rectangle $0 < x < L$, $0 < t < t_f$. If the roles of the independent variables are reversed, i.e., if x is regarded as the "time" variable and t as the "space" variable, then system (6) is identical to the system

*If the final time temperature distribution is known, it should certainly be used for $T_1(x)$. In this case, computations in the shaded region of Fig. 2 would produce legitimate temperature values.

ORNL - DWG 80-12983

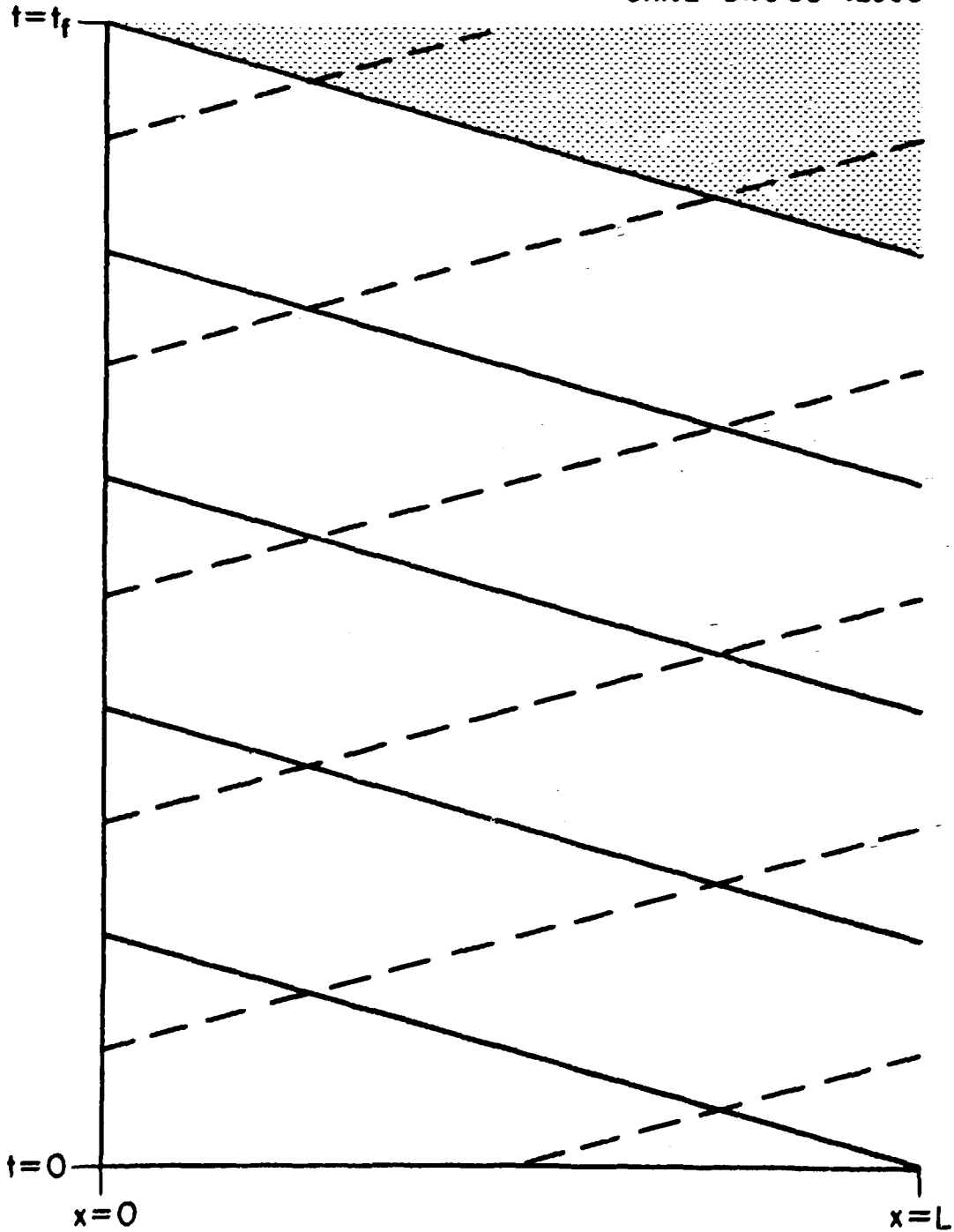


Fig. 2. Characteristic Curves of Modified System

$$\alpha \frac{\partial^2 u}{\partial \tau^2} - \gamma \frac{\partial^2 u}{\partial \xi^2} - \frac{\partial u}{\partial \xi} = 0 \quad 0 < \xi < t_f, \quad 0 < \tau < L \quad (7a)$$

$$u(\xi, 0) = f(\xi) \quad (7b)$$

$$\frac{\partial u}{\partial \tau}(\xi, 0) = g(\xi) \quad (7c)$$

$$u(0, \tau) = T_0(\tau) \quad (7d)$$

$$u(t_f, \tau) = T_1(\tau), \quad (7e)$$

where ξ is considered the space variable and τ the time variable. System (7) is a conventional initial-boundary value problem for a second order hyperbolic equation with constant coefficients. Tychonov and Samarski [11, pp. 107-116] use the Riemann function to derive a closed form solution for this system which is analogous to the D'Alembert solution for the undamped wave equation. The qualities of existence, uniqueness, and continuous dependence on data follow easily from this solution; hence, system (7) represents a well-posed problem.

In summary, the inverse heat conduction problem (1) can be closely approximated by the hyperbolic system (6). If viewed as in system (7), this hyperbolic system is well-posed; hence, the unstable nature and possible data incompatibility are completely overcome. Another advantage of this procedure, to be developed later, is that the numerical solution of the approximating hyperbolic system is efficient and accurate, even for nonlinear problems.

IV. SAMPLE PROBLEMS

To further examine this approach, three test problems are considered. All are similar in form to system (1) and have known analytic solutions.

Problem I. Slab geometry, constant properties. This example is used to demonstrate the accuracy that can be obtained for linear problems. For simplicity, the spatial variable is restricted to the interval $0 \leq x \leq 1$ and the physical constants k, α are unity. Boundary conditions model an insulated boundary at $x = 0$ and a specified temperature at $x = x''$. Because these conditions are not given at the same point, this problem is well-posed in the region $0 < x < x''$; the formulation in the region $x'' < x < 1$ constitutes an inverse problem. To simplify notation, let $u = u(x, t)$ denote the well-posed solution ($0 < x < x''$), so that $T(x, t)$ represents only the inverse solution ($x'' < x < 1$). Both u and T must satisfy the heat conduction equation (1a) and the initial condition (1d) in their respective regions; each must also satisfy the boundary condition (1b). The equation

$$\frac{\partial u}{\partial x}(0, t) = 0$$

is the second boundary condition for the well-posed solution u . The second condition [cf. Eq. (1c)] for T is obtained by applying continuity of heat flux (conservation of energy) at x'' ; this leads to

$$\frac{\partial u}{\partial x}(x'', t) = \frac{\partial T}{\partial x}(x'', t), \quad 0 < t < t_f. \quad (8)$$

Upon solution of the well-posed problem, Eq. (8) constitutes known boundary data for the ill-posed problem.

An exact solution should vary significantly in both variables, in order to thoroughly test the solution method. It should also have a simple form, to facilitate the analysis. Selecting the exact solution in both regions to be

$$T(x, t) = \cos x e^{\beta t} \quad (9)$$

and substituting into Eqs. (1a), (1b), and (1d), the functions Q , f , and T_0 are determined to be

$$Q(x,t) = (1 + \beta) \cos x e^{\beta t} \quad (10)$$

$$T_0(x) = \cos x \quad (11)$$

$$f(t) = \cos x e^{\beta t} \quad (12)$$

A numerical solution is obtained using Eqs. (10)-(12) as data in both the well-posed and inverse regions. This solution is then compared with Eq. (9) for validation.

Problem II. Slab geometry, highly nonlinear. This example, representing heat conduction with a nonlinear source term, is adapted from Ref. 4. Eq. (1a) is replaced by

$$\frac{\partial T}{\partial t} - \frac{\partial^2 T}{\partial x^2} = (1 + T^2)(1 - 2T), \quad 0 < x < 1, \quad 0 < t < t_f, \quad (13)$$

which is solved using the auxiliary conditions (1b)-(1d) with $x'' = 0$, $f(t) = \tan t$, $g(t) = 1 + \tan^2 t$, and $T_0(x) = \tan x$. A numerical solution is obtained and then compared with the exact solution

$$T(x,t) = \tan(x + t). \quad (14)$$

Problem III. Radial geometry, nonlinear, inhomogeneous material. This problem is similar to that encountered in evaluating the heat transfer properties of nuclear reactor fuel rods. A cylinder composed of two materials arranged in concentric regions has the temperature specified at the interface. For simplicity, the radii of the interface and outer boundary are specified as $r = \frac{1}{2}$ and $r = 1$, respectively. Assuming heat conduction only in the radial dimension, the temperature in each region satisfies the equation

$$\rho C_p(T) \frac{\partial T}{\partial t} - \frac{1}{r} \frac{\partial}{\partial r} \left[r k(T) \frac{\partial T}{\partial r} \right] = Q(r, t). \quad (15)$$

The initial temperature and the inner wall temperature at $r = \frac{1}{2}$ are also specified, corresponding to conditions (1b) and (1d). Since the problem is independent of azimuthal angle, the boundary condition

$$\left. \frac{\partial T}{\partial r} \right|_{r=0} = 0 \quad (16)$$

is imposed, which, as in Problem I, creates a well-posed problem in the inner region. Upon solution in this region, the continuity of heat flux provides the following interface condition:

$$\left[k(T) \frac{\partial T}{\partial r} \right]_{r=\frac{1}{2}^+} = \left[k(T) \frac{\partial T}{\partial r} \right]_{r=\frac{1}{2}^-}, \quad (17)$$

which is the second boundary condition for the outer (ill-posed) region. This corresponds to Eq. (8) in Problem I, and can easily be put in the form of Eq. (1c).

Exact solutions and physical coefficients are chosen to be of the form

$$T(r, t) = \begin{cases} (2 - 5r^2) e^{\beta t} & r < \frac{1}{2} \\ \eta \cos r e^{\beta t} & r > \frac{1}{2} \end{cases}, \quad (18)$$

$$k(T) = \begin{cases} \nu(1 + T) & r < \frac{1}{2} \\ 1 + T & r > \frac{1}{2} \end{cases}, \quad \rho C_p(T) = \begin{cases} \frac{1}{2} (20 - T) & r > \frac{1}{2} \\ \frac{1}{10} (10 - T) & r < \frac{1}{2} \end{cases}.$$

Analogous to the development of Problem I, these representations are substituted into Eqs. (15), (1d), and (1b) to obtain the heat source and initial temperatures for each region as well as the interface temperature $f(t)$. As described in both previous examples, this "physical data" is used to compute a numerical solution, which is then compared with Eq. (18) for verification.

V. NUMERICAL APPROXIMATIONS

When data is given at two distinct spatial points, as in *Problems I* and *III*, temperatures in the well-posed region are determined at all time steps before the solution in the ill-posed region is begun. This results in an explicit representation for the interface flux, which is necessary for the solution of the inverse problem. To obtain a discrete approximation in the well-posed region, any numerical method for parabolic equations can be used. The Crank-Nicolson implicit scheme is used for both *Problems I* and *III* in this article, giving excellent results. Details of the method can be found in standard texts on numerical analysis;* hence, it will not be discussed further in this study.

In order to solve the inverse problems (ill-posed regions of *Problems I* and *III*, entire slab for *Problem II*) by the method presented in Sect. III, it is necessary to add the term $\gamma(\partial^2 T/\partial t^2)$ to the left-hand sides of Eqs. (1a), (13), and (15). The resulting differential equations can then be discretized by any conventional method for hyperbolic equations. Consistent with the discussion accompanying system (7), the numerical solution is obtained for all time steps at a given spatial node before any temperature values are computed at the next spatial node. This is in contrast to solution methods for the direct problem, which generally solve for all spatial nodes at a given time step before computing any values at the next time step.

As an illustration of the solution procedures used for all three inverse problems, consider the modified equation for the ill-posed region of *Problem I*,

*See, for example, Ames [12] or Forsythe and Wasow [13].

$$\gamma \frac{\partial^2 T}{\partial t^2} + \frac{\partial T}{\partial t} - \frac{\partial^2 T}{\partial x^2} = Q(x, t) \quad x'' < x < 1, \quad 0 < t < t_f. \quad (19)$$

Introducing the discrete mesh (x_i, t_k) and using the customary notation $T(x_i, t_k) = T_{i,k}$, Eq. (19) is discretized using central differences to approximate all derivatives. This results in the following second-order, explicit difference equation:

$$\begin{aligned} & \frac{\gamma}{(\Delta t)^2} (T_{i,k+1} - 2T_{i,k} + T_{i,k-1}) + \frac{1}{2\Delta t} (T_{i,k+1} - T_{i,k-1}) \\ & = \frac{1}{(\Delta x)^2} (T_{i+1,k} - 2T_{i,k} + T_{i-1,k}) + Q(x_i, t_k) \\ & + O[(\Delta x)^2 + (\Delta t)^2]. \end{aligned} \quad (20)$$

Eq. (20) is tri-level, since temperature values from three different spatial positions appear. It is explicit because only one temperature value at the unknown spatial position x_{i+1} is involved. Courant, Fredricks, and Levy [14] have shown that this difference equation is convergent (numerically stable and consistent) to the differential equation (19) provided the inequality

$$\gamma \frac{(\Delta x)^2}{(\Delta t)^2} \leq 1 \quad (21)$$

is satisfied. In practice, this condition poses virtually no restriction at all, since γ must be very small from previous considerations.

The discretization of Problems II and III follows closely the previous discussion for Problem I. As in Eq. (20), the difference equations for these problems are also second-order explicit and tri-level. For Problem II, solution is restricted to the region where $x + t < \pi/2$ since the exact solution (14) becomes infinite if this condition is violated. Were the problems linear, numerical stability would occur when Eq. (21) holds for Problem II and when

$$\frac{\gamma (\Delta x)^2}{k (\Delta t)^2} \leq 1 \quad (22)$$

holds for *Problem III* [14]. Although stability conditions for the actual nonlinear problems are not known, Eqs. (21) and (22) were easily satisfied (since γ must be very small) and no computations showed any sign of instability.

VI. COMPUTATION RESULTS

Computer programs have been written implementing the numerical schemes of the previous section for each of the three sample problems. The exact solutions were also computed and compared with the difference solutions. Results reported here for all three problems were calculated using a value of $\gamma = 0.01$, although all runs with $\gamma < 0.01$ gave virtually identical results.

The calculated results from all three sample problems showed good accuracy when compared with the exact solutions. As depicted in Table 1, the spatial profiles of discrete temperatures for *Problem III* showed slightly increasing error moving away from the node where data was given. This error, due to discretization and roundoff, is to be expected. It does not provoke unstable solution behavior, as even the temperature values near the outer surface retain considerable accuracy.

To illustrate the time behavior of the solutions, Tables 2-6 compare the surface temperatures and heat fluxes with the exact values for each problem. At each time step, the surface heat flux was computed from the temperature distribution using the following second-order, backward difference approximation for the temperature derivative:

$$\left(\frac{\partial T}{\partial x}\right)_{i,k} = \frac{1}{2\Delta x} \left[3T_{i,k} - 4T_{i-1,k} + T_{i-2,k} \right] + O[(\Delta x)^2]. \quad (23)$$

Table 1. Problem III Radial Profile Comparison^a of Calculated and Exact
Temperatures Solution at Selected Time Values^b

Time	Radial Values										
	0.50	0.55	0.60	0.65	0.70	0.75	0.80	0.85	0.90	0.95	1.00
1.5	1.5877	1.5422	1.4928	1.4397	1.3830	1.3228	1.2593	1.1927	1.1231	1.0506	0.9755
	1.5877	1.5424	1.4932	1.4403	1.3838	1.3238	1.2605	1.1941	1.1246	1.0524	0.9775
3.0	3.3612	3.2646	3.1599	3.0473	2.9270	2.7994	2.6648	2.5235	2.3758	2.2221	2.0628
	3.3612	3.2652	3.1611	3.0491	2.9294	2.8024	2.6684	2.5278	2.3808	2.2279	2.0694
4.5	7.1156	6.9109	6.6889	6.4502	6.1953	5.9248	5.6394	5.3398	5.0267	4.7008	4.3629
	7.1156	6.9124	6.6920	6.4548	6.2015	5.9327	5.6490	5.3513	5.0401	4.7164	4.3809

^aTop line is calculated; bottom line is exact solution.

^bUses parameter value $\beta = 0.5$.

Table 2. Problem I Surface Calculations^a

Time	Calculated Temperature	Exact Temperature	Relative Error ^b	Calculated Flux	Exact Flux	Relative Error ^b
0.0	0.5403	0.5403	0.0000	0.8422	0.8415	-0.0008
0.5	0.4207	0.4208	0.0001	0.6557	0.6553	-0.0005
1.0	0.3277	0.3277	0.0001	0.5106	0.5104	-0.0005
1.5	0.2552	0.2552	0.0001	0.3977	0.3975	-0.0005
2.0	0.1987	0.1988	0.0001	0.3097	0.3096	-0.0005
2.5	0.1548	0.1548	0.0001	0.2412	0.2411	-0.0005
3.0	0.1205	0.1206	0.0001	0.1879	0.1878	-0.0005
3.5	0.0939	0.0939	0.0001	0.1463	0.1462	-0.0005
4.0	0.0731	0.0731	0.0001	0.1139	0.1139	-0.0005
4.5	0.0569	0.0569	0.0002	0.0887	0.0887	-0.0005

^aUses parameter values $\beta = -0.5$, $x'' = 0.5$

^bRelative Error = (Exact - Calculated)/Exact

Table 3. Problem II Surface Calculations

Time	Calculated Temperature	Exact Temperature	Relative Error ^a	Calculated Flux	Exact Flux	Relative Error ^a
0.00	1.5574	1.5574	0.0000	-3.4151	-3.4255	0.0030
0.05	1.7523	1.7433	-0.0052	-4.0731	-4.0391	-0.0084
0.10	1.9762	1.9648	-0.0058	-4.9037	-4.8603	-0.0089
0.15	2.2492	2.2345	-0.0066	-6.0482	-5.9930	-0.0092
0.20	2.5915	2.5722	-0.0075	-7.6874	-7.6160	-0.0094
0.25	3.0357	3.0096	-0.0087	-10.148	-10.057	-0.0090
0.30	3.6383	3.6021	-0.0100	-14.082	-13.975	-0.0076
0.35	4.5080	4.4552	-0.0118	-20.938	-20.849	-0.0043
0.40	5.8797	5.7979	-0.0141	-34.471	-34.615	0.0042
0.45	8.3735	8.2380	-0.0165	-66.990	-68.865	0.0272
0.50	14.280	14.101	-0.0127	-178.45	-199.84	0.1071
0.52	19.651	19.669	0.0009	-312.67	-387.88	0.1939
0.54	30.7159	32.4601	0.0537	-656.75	-1054.7	0.3773
0.56	62.088	92.616	0.3296	-1899.0	-8578.1	0.7786

^aRelative Error = (Exact - Calculated)/Exact

Table 4. Problem III Surface Calculations with
Exponential Decrease in Exact Solution^a

Time	Calculated Temperature	Exact Temperature	Relative Error ^b	Calculated Flux	Exact Flux	Relative Error ^b
0.0	0.4618	0.4618	0.0000	1.0521	1.0512	-0.0008
0.5	0.3593	0.3596	0.0009	0.7627	0.7615	-0.0016
1.0	0.2798	0.2801	0.0010	0.5592	0.5583	-0.0016
1.5	0.2179	0.2181	0.0010	0.4144	0.4138	-0.0016
2.0	0.1697	0.1699	0.0010	0.3100	0.3095	-0.0015
2.5	0.1322	0.1323	0.0009	0.2336	0.2333	-0.0014
3.0	0.1029	0.1030	0.0008	0.1772	0.1770	-0.0013
3.5	0.0802	0.0802	0.0007	0.1352	0.1350	-0.0012
4.0	0.0625	0.0625	0.0007	0.1035	0.1034	-0.0011
4.5	0.0486	0.0487	0.0006	0.0796	0.0795	-0.0011
5.0	0.0379	0.0379	0.0005	0.0613	0.0613	-0.0006

^aUses parameter values $\beta = -0.5$, (exponential decrease in time)

^bRelative Error = (Exact - Calculated)/Exact

Table 5. Problem III Surface Calculations with
Exponential Increase in Exact Solution^a

Time	Calculated Temperature	Exact Temperature	Relative Error ^b	Calculated Flux	Exact Flux	Relative Error ^b
0.0	0.4618	0.4618	0.0000	1.0521	1.0512	-0.0008
0.5	0.5922	0.5929	0.0011	1.4737	1.4709	-0.0019
1.0	0.7601	0.7613	0.0016	2.0934	2.0883	-0.0024
1.5	0.9750	0.9775	0.0021	3.0193	3.0106	-0.0029
2.0	1.252	1.255	0.0025	4.4228	4.4084	-0.0033
2.5	1.607	1.612	0.0028	6.5791	6.5553	-0.0036
3.0	2.063	2.069	0.0032	9.9319	9.8924	-0.0040
3.5	2.648	2.657	0.0035	15.200	15.134	-0.0043
4.0	3.399	3.412	0.0038	23.551	23.443	-0.0046
4.5	4.363	4.381	0.0041	36.891	36.713	-0.0049
5.0	5.601	5.625	0.0043	58.336	58.040	-0.0051

^aUses parameter values $\beta = 0.5$, (exponential increase in time)

^bRelative Error = (Exact - Calculated)/Exact

Table 6. Problem II Surface Temperature Results with Perturbed Data

Time	Calculated Temperature ^a			Exact Temp.	Relative Error ^{a, b}		
	1	2	3		1	2	3
0.00	1.5599	1.5574	1.5574	1.5574	-0.0016	0.0000	0.0000
0.05	1.6890	1.7077	1.7523	1.7433	0.0312	0.0204	-0.0052
0.10	1.9948	2.0170	1.9762	1.9648	-0.0153	-0.0266	-0.0058
0.15	2.2036	2.2327	2.2492	2.2345	0.0138	0.0008	-0.0066
0.20	2.6514	2.5955	2.5915	2.5722	-0.0308	-0.0091	-0.0075
0.25	3.2652	3.0447	3.0357	3.0096	-0.0849	-0.0117	-0.0087
0.30	3.7952	3.6707	3.6383	3.6021	-0.0536	-0.0191	-0.0100
0.35	4.2172	4.4563	4.5080	4.4552	0.0534	-0.0002	-0.0118
0.40	5.8334	5.7487	5.8797	5.7979	-0.0061	0.0085	-0.0141
0.45	8.3735	8.6286	8.3735	8.2380	-0.0164	-0.0474	-0.0165
0.50	15.455	14.043	14.280	14.101	-0.0960	0.0041	-0.0127
0.52	17.543	19.018	19.651	19.669	0.1081	0.0331	0.0009
0.54	34.404	28.232	30.716	32.460	-0.0599	0.1302	0.0537
0.56	59.598	54.682	62.088	92.616	0.3565	0.4096	0.3296

^aCase 1: Both boundary and initial conditions subject to maximum of 3% random error

Case 2: Flux boundary condition subject to maximum of 3% random error

Case 3: Exact boundary and initial conditions

^bRelative Error = (Exact - Calculated)/Exact

As expected, the computed solution for *Problem I* (constant properties) shows better agreement than the calculations for either nonlinear problem. However, even the nonlinear problem results show accuracy to within 2% for most values.

Another observation concerns the decreasing accuracy of the computations for problems where the exact solutions are increasing with time. As shown in Table 5, *Problem III* calculations with a positive exponential parameter β [cf. Eq. (18)] are not as accurate as those for negative β . Similarly, Table 3 indicates that the numerical results for *Problem II* are worthless in the immediate vicinity of the boundary $x + t = \pi/2$. However, no numerical approximation could be expected to perform reliably near a point where the solution becomes infinite. In the final analysis, this type of behavior is to be expected for problems with increasing solutions; hence, neither of these results is unreasonable.

It is important to emphasize that the inverse computations of *Problems I* and *III* must use the results from their well-posed regions to calculate interface data. This involves the approximation of Eq. (23) to calculate the interface flux. The approximate nature of this data shows little adverse effect on the inverse solution as a whole, since in each case the differential formulation [corresponding to system (6)] is well-posed and the numerical approximation is stable. This favorable quality of the solution methodology is further illustrated in Table 6. These results are obtained by solving *Problem II* with randomly perturbed data. To achieve this, uniformly distributed random errors between $\pm 3\%$ were introduced at each point in the values of the functions f , g , and T_0 . As seen in Table 6, these random errors are propagated as slight inaccuracies in the surface temperatures, but not as vicious oscillation or unbounded growth.

VII. SUMMARY AND CONCLUSIONS

The analysis of the linear inverse formulation in Sect. II showed that the exact solution of Eq. (2) is characterized by discontinuous dependence on data (instability). Nevertheless, most previous solution procedures have utilized a direct approach, and certain of these methods have obtained reasonable solution results for some cases. However, the ill-posed nature of the problem implies that direct solution procedures are not capable of consistently producing reliable results.

In order to be assured of a meaningful solution, it was useful to actually change the form of the problem and to alter one's perspective of the problem. Thus, the heat conduction operator was approximated by a hyperbolic equation, and was solved numerically for all time steps at each spatial node before progressing to the next spatial node. Although this violates a fundamental principle of direct heat conduction (namely, temperatures at a given time do not depend on temperature values at any future time), it was seen to be a significant factor in devising a solution methodology for the inverse problem. Of particular importance in this approach was the introduction of the coefficient γ [cf. Eq. (6a)], which was required to be small in order to

- i) assure that the governing equation accurately described heat conduction,
- ii) reduce the domain of influence of the added final time condition, and
- iii) maintain numerical stability.

The formulation presented in Sect. III utilized all of these ingredients to produce a well-posed problem that closely approximated the original inverse problem.

The new solution method was applied to several test problems and the resulting solutions were in good agreement with the known exact solutions. The procedure was applicable to nonlinear problems and to problems involving several material regions. The numerical solution was obtained efficiently and quickly by an explicit, second order algorithm; solution stability was maintained with insignificant restrictions on stepsizes, even for randomly perturbed data. Thus, the method appears applicable to virtually any formulation of this inverse heat conduction problem.

26

REFERENCES

1. O. R. Burggraf, "An Exact Solution of the Inverse Problem in Heat Conduction Theory and Applications," J. Heat Transfer, **86C**, 373-382 (1964).
2. E. M. Sparrow, A. Haji-Sheikh, and T. S. Lundgren, "The Inverse Problem in Transient Heat Conduction," J. Appl. Mech., **86E**, 369-375 (1964).
3. J. V. Beck, "Nonlinear Estimation Applied to the Nonlinear Inverse Heat Conduction Problem," Int. J. Heat Mass Transfer, **13**, 703-716 (1970).
4. L. Garifo, V. E. Schrock, and E. Spedicato, "On the Solution of the Inverse Heat Conduction Problem by Finite Differences," Energia Nucleare, **22**, 452-464 (1975).
5. L. J. Ott and R. A. Hedrick, "ORINC - A One-Dimensional Implicit Approach to the Inverse Heat Conduction Problem," ORNL/NUREG-23, Oak Ridge National Laboratory (1977).
6. B. R. Bass, "INCAP, A Finite Element Program for One-Dimensional Nonlinear Inverse Heat Conduction Analysis," ORNL/NUREG/CSD/TM-8, Oak Ridge National Laboratory (1979).
7. A. N. Tikhonov and V. Y. Arsenin, Solutions of Ill-Posed Problems, Winston/Wiley, Washington (1977).
8. D. V. Widder, The Heat Equation, Academic Press, New York (1975).
9. P. J. Roache, Computational Fluid Dynamics, Hermosa, Albuquerque (1976).
10. M. Morse and R. Feshbach, Methods of Theoretical Physics, McGraw-Hill (1953).
11. A. N. Tychonov and A. A. Samarski, Partial Differential Equations of Mathematical Physics, Holden-Day, San Francisco (1964).
12. W. F. Ames, Numerical Methods for Partial Differential Equations, Academic Press, New York (1977).
13. G. E. Forsythe and W. R. Wasow, Finite Difference Methods for Partial Differential Equations, Wiley, New York (1960).
14. R. Courant, K. Fredricks, and H. Lewy, "On the Partial Differential Equations of Mathematical Physics," IBM Journal, March 1967, 215-234 (1967). [Translation of article first published in Mathematische Annalen, **100**, 32-74 (1928).]

15. P. R. Garabedian, Partial Differential Equations, Wiley, New York (1964).
16. F. John, Partial Differential Equations, Springer-Verlag, New York (1978).

APPENDIX

Taking the difference of the functions T_1 and T_2 in Eq. (5) results in

$$\begin{aligned} T_1 - T_2 &= \sum_{n=0}^{\infty} \frac{1}{(2n)!} \left(\frac{x^2}{\alpha}\right)^n \frac{d^n}{dt^n} \left(\frac{1}{\beta} \cos \beta^2 t\right) \\ &= \frac{1}{\beta} \sum_{n=0}^{\infty} \frac{(-1)^n}{(4n)!} \left(\frac{x^2}{\alpha}\right)^n \beta^{4n} \cos \beta^2 t \\ &\quad + \frac{1}{\beta} \sum_{n=0}^{\infty} \frac{(-1)^{n+1}}{(4n+2)!} \left(\frac{x^2}{\alpha}\right)^{2n+1} \beta^{4n+2} \sin \beta^2 t. \end{aligned}$$

For $t = 0$, $x^2 = \alpha$, the above reduces to

$$T_1 - T_2 = \frac{1}{\beta} \sum_{n=0}^{\infty} \frac{(-1)^n}{(4n)!} \beta^{4n},$$

and therefore

$$\|T_1 - T_2\| = \max_{\substack{0 \leq t \leq t_f \\ 0 \leq x \leq L}} |T_1(x, t) - T_2(x, t)| \geq \frac{1}{\beta} \left| \sum_{n=0}^{\infty} \frac{(-1)^n}{(4n)!} \beta^{4n} \right|. \quad (\text{A.1})$$

A closed form for the series on the right can be obtained as follows:

$$\begin{aligned} \cosh \mu \cos \mu &= \frac{1}{4} (e^{\mu} + e^{-\mu})(e^{i\mu} + e^{-i\mu}) \\ &= \frac{1}{4} \left[e^{\mu(1+i)} + e^{\mu(1-i)} + e^{\mu(i-1)} + e^{\mu(-1-i)} \right] \\ &= \frac{1}{4} \sum_{n=0}^{\infty} \frac{\mu^n}{n!} \left[(1+i)^n + (1-i)^n + (-1)^n (1-i)^n + (-1)^n (1+i)^n \right] \\ &= \frac{1}{2} \sum_{n=0}^{\infty} \frac{\mu^{2n}}{(2n)!} \left[(1+i)^{2n} + (1-i)^{2n} \right]. \end{aligned} \quad (\text{A.2})$$

Substituting the equalities

$$1 + i = \sqrt{2} e^{i\pi/4} = \sqrt{2}i, \quad 1 - i = \sqrt{2} e^{-i\pi/4} = \sqrt{-2}i$$

into Eq. (A.2) gives

$$\begin{aligned} \cosh \mu \cos \mu &= \frac{1}{2} \sum_{n=0}^{\infty} \frac{\mu^{2n}}{(2n)!} \left[(2i)^n + (-1)^n (2i)^n \right] \\ &= \sum_{n=0}^{\infty} \frac{\mu^{4n}}{(4n)!} (2i)^{2n} \\ &= \sum_{n=0}^{\infty} \frac{(\sqrt{2}\mu)^{4n}}{(4n)!} (-1)^n. \end{aligned}$$

Letting $\beta = \sqrt{2} \mu$ gives

$$\cosh \frac{\beta}{\sqrt{2}} \cos \frac{\beta}{\sqrt{2}} = \sum_{n=0}^{\infty} \frac{(-1)^n}{(4n)!} \beta^{4n},$$

which is the desired result.